Research Square

Preprints are preliminary reports that have not undergone peer review.
They should not be considered conclusive, used to inform clinical practice,
or referenced by the media as validated information.

The RING-type E3 ubiquitin ligase CgrUbr1 regulates vegetative growth, hyphal morphology, asexual development, and pathogenicity in Colletotrichum graminicola

Sheng Li
Hainan University
Min Li
Hainan University
Zhihui He
Hainan University
Qin Lei
Hainan University
Zhiqiang Liu
liuzhiqiang80@126.com
Hainan University https://orcid.org/0000-0003-3077-638X
Xiaoyu Li
Hainan University

Research Article

Keywords: Colletotrichum graminicola, E3 ubiquitin ligase, morphogenesis, asexual development, pathogenicity

Posted Date: November 9th, 2026

DOI: https://doi.org/10.21203/rs.3.rs-11342592/v1

License: This work is licensed under a Creative Commons Attribution 4.0 International License.
Read Full License

Abstract

Colletotrichum graminicola is a significant phytopathogenic fungus responsible for maize anthracnose. Ubr1 functions as a critical RING-type E3 ubiquitin ligase within the N-degron pathway; however, its specific role in *Colletotrichum* species remains poorly understood. In this study, we characterized the Ubr1 homolog, CgrUbr1, in *C. graminicola*. Bioinformatics analysis revealed that CgrUbr1 possesses the canonical zf-UBR, ClpS, and RING domains. Disruption of *Cgrubr1* resulted in a significantly reduced growth rate, distinct segmental swelling, a characteristic bead-like hyphal morphology, and a higher frequency of septation. Regarding asexual development, the Δ*Cgrubr1* mutants exhibited a severe reduction in the yield of both oval and falcate conidia, both of which displayed pronounced morphological defects. Furthermore, oval conidia exhibited negligible germination rates, while falcate conidia were unable to differentiate into typical appressoria. Pathogenicity assays confirmed that *Cgrubr1* deletion drastically attenuated virulence on maize leaves, failing to produce visible lesions on intact tissue. Transcriptomic profiling revealed significant dysregulation of genes involved in DNA replication, chitin metabolism, and infection-related pathways in the mutant strain. Collectively, these findings demonstrate that CgrUbr1 is indispensable for vegetative growth, hyphal morphogenesis, asexual reproduction, and pathogenicity in *C. graminicola*.

1 Introduction

Maize (*Zea mays* L.) serves as a globally vital food and feed crop, as well as a key raw material for food processing and diverse industrial applications (Ranum et al., 2014). Within the genus *Colletotrichum*, species exhibit broad host ranges and varied infection strategies, ranking them among the most significant groups of plant-pathogenic fungi (Dean et al., 2012). Specifically, *Colletotrichum graminicola* stands as a primary causal agent of maize anthracnose, inciting systemic infections that compromise the leaves, stalks, and roots (Rudolph et al., 2025; Sukno et al., 2008). Leaf and stalk infections manifest as anthracnose leaf blight and stalk rot, respectively; severe cases often lead to stalk lodging and substantial yield losses (Bergstrom & Nicholson, 1999). *C. graminicola* is characterized as a typical hemibiotrophic fungus. It initially colonizes living host cells in a biotrophic manner before transitioning to a necrotrophic phase (Mims & Vaillancourt, 2002). This shift is marked by dynamic changes in infection-related gene expression, host tissue necrosis, and the development of characteristic anthracnose lesions (O'Connell et al., 2012). The pathogen produces two morphologically and developmentally distinct asexual conidial types: falcate and oval conidia (Panaccione et al., 1989). Falcate conidia, primarily formed in acervuli within leaf lesions, function as key propagules for dissemination and secondary infection (Bergstrom & Nicholson, 1999). Upon encountering the host surface, these conidia germinate to form melanized appressoria, which then generate penetration pegs to breach the epidermis, followed by the development of primary and secondary invasive hyphae (Mims & Vaillancourt, 2002). Conversely, oval conidia are mainly produced by hyphae in infected tissues; their germlings display a high frequency of hyphal fusion, forming interconnected networks that are closely associated with the infection process (Nordzieke et al., 2019). Collectively, these two conidial types exhibit distinct differences in morphology, formation, germination behavior, and infection characteristics.

During host infection, pathogenic fungi must dynamically modulate their growth, differentiation, and stress responses to accommodate environmental changes. These adaptive processes are governed not only by transcriptional regulation and signal transduction but also by precise post-translational control of key protein activity and stability. The ubiquitin-proteasome system (UPS) is central to protein homeostasis, selectively regulating intracellular protein abundance and participating in diverse cellular processes (Finley et al., 2012). Ubiquitination is executed sequentially by E1 ubiquitin-activating enzymes, E2 ubiquitin-conjugating enzymes, and E3 ubiquitin ligases. Among these, E3 ligases confer substrate specificity by recognizing target proteins (Zheng & Shabek, 2017). Distinct ubiquitination topologies dictate different substrate fates: K48-linked polyubiquitin chains predominantly earmark proteins for proteasomal degradation, whereas non-K48-linked polyubiquitination and monoubiquitination are frequently engaged in non-proteolytic regulation, such as DNA repair and membrane protein trafficking (Finley et al., 2012). Accumulating evidence indicates that the UPS broadly participates in fungal morphogenesis, stress adaptation, host interaction, and pathogenicity (Cao & Xue, 2021). In *Magnaporthe oryzae*, SCF-associated F-box proteins, including MoFwd1, MoCdc4, and MoFbx15, are required for hyphal growth, conidiation, and virulence (Shi et al., 2019). Similarly, the F-box protein MoGrr1 contributes to stress responses and pathogenicity by modulating the homeostasis of oxidative stress-related proteins (Li et al., 2020). In *Verticillium dahliae*, disruption of the RING (Really Interesting New Gene) -type E3 ligases VdBre1 or VdHrd1 compromises infection structure formation, vascular colonization, and pathogenicity (Yang et al., 2023). These findings underscore the widespread involvement of E3 ubiquitin ligases in regulating growth, development, and infectivity across plant-pathogenic fungi.

Ubr1 is a canonical N-recognin and RING-type E3 ligase in the N-degron pathway that mediates substrate degradation (Tasaki et al., 2012; Zheng & Shabek, 2017). It employs a UBR-box for basic type I N-degrons (Arg/Lys/His) and an N-domain for bulky hydrophobic type II N-degrons (Phe/Trp/Tyr/Leu/Ile), with its RING domain driving ubiquitin transfer (Xia et al., 2008). Beyond direct recognition, Ubr1 activity is fine-tuned by nutrient cues and enzymatic cooperation. In *Saccharomyces cerevisiae*, dipeptides enhance its recognition of the repressor Cup9 to regulate peptide transporter (*PTR2*) expression (Du et al., 2002; Turner et al., 2000), and collaboration with the HECT ligase Ufd4 promotes efficient K48-linked polyubiquitination (Hwang et al., 2010). Ubr1 homologs have been functionally characterized in several fungal species, revealing their conserved and divergent roles in development and pathogenesis. In *Fusarium verticillioides*, deletion of *Ubl1* (a *Ubr1* homolog) causes defects in conidiation, hyphal morphology, and pigment deposition, while reducing colonization of maize kernels. *Ubl1* also physically interacts with the Gα subunits Gpa1 and Gpa2, suggesting its involvement in sensing extracellular nutrient signals (Ridenour et al., 2014). In *Beauveria bassiana*, disruption of *BbUbr1* leads to impaired polarized growth, decreased conidial production, altered cell wall properties, and a significant attenuation of virulence (Wang et al., 2021). In *M. oryzae*, the MoRad6-mediated ubiquitination pathway engages the E3 ligase MoUbr1 and is required for conidial germination, infection-related morphogenesis, and pathogenicity (Shi et al., 2016). Overall, these findings establish that Ubr1 homologs and their

associated ubiquitination pathways play pivotal roles in regulating hyphal growth, asexual development, cell wall homeostasis, and pathogenicity across diverse fungi.

To date, the biological function of Ubr1 in the genus *Colletotrichum* remains unexplored. In this study, we generated *Cgrubr1* deletion mutants to systematically investigate the role of CgrUbr1 in *C. graminicola*. We assessed the effects of *Cgrubr1* deletion on vegetative growth, hyphal morphology, asexual development, conidial germination, appressorium formation, and pathogenicity. Furthermore, transcriptome profiling was conducted to identify differentially expressed genes and altered biological processes upon *Cgrubr1* loss, aiming to elucidate the molecular basis of CgrUbr1 in fungal development and host infection.

2 Materials and Methods

2.1 Fungal strains and culture conditions

C. graminicola strain CgM2, used as the wild-type (WT) in this study, was maintained in the School of Life and Health Sciences, Hainan University (Wang et al., 2025). The media used in this study included potato dextrose agar (PDA), potato dextrose broth (PDB), complete medium (CM), minimal medium (MM), Czapek medium (CZ), oatmeal agar (OMA), and regeneration medium (RGM). All media were prepared according to protocols established in our laboratory (Lin et al., 2025; Zhang et al., 2024).

2.2 Sequence analysis of *Cgrubr1*

The *Cgrubr1* gene and its encoded protein sequence were retrieved from the NCBI database based on the *C. graminicola* reference genome (GenBank accession: GCF_000149035.1). Conserved domains within CgrUbr1 were predicted using the SMART online tool. To assess evolutionary relationships, protein sequences of Ubr1 homologs from various fungal species were obtained from GenBank and aligned using ClustalW. A phylogenetic tree was then constructed with MEGA 6.0 using the neighbor-joining (NJ) method with bootstrap values calculated from 1,000 replicates, to evaluate the phylogenetic placement of CgrUbr1 among fungal Ubr1 homologs.

2.3 Gene knockout and complementation

Cgrubr1 knockout mutants were constructed by homologous recombination. Genomic DNA from CgrWT was used as the template to amplify the upstream and downstream homologous regions of *Cgrubr1* with the primer pairs *Cgrubr1*UF/*Cgrubr1*UR and *Cgrubr1*DF/*Cgrubr1*DR, respectively. The amplified fragments were ligated into the pUC18-HPT vector to generate the gene knockout construct. After sequence verification and linearization, the construct was introduced into CgrWT protoplasts. Hygromycin-resistant transformants were selected and verified by PCR using the primer pairs *Cgrubr1*F/*Cgrubr1*R, *Cgrubr1*UU/PI, and *Cgrubr1*DD/PI1. For complementation, a *Cgrubr1* genomic fragment containing its native promoter region was amplified from CgrWT genomic DNA and inserted into the pUC18-G418 vector. The resulting construct was introduced into Δ*Cgrubr1* protoplasts. G418-resistant transformants

were selected and verified by PCR using Cgrubr1F/Cgrubr1R. The sequences of all primers used in this study are listed in Table S1.

2.4 Vegetative growth and hyphal morphology

For growth assays, 5-mm mycelial plugs were taken from the leading edges of actively growing colonies and transferred to PDA, CM, MM, CZ, and OMA media. All strains were incubated at 28°C for 5 days. Colony diameter was measured in two perpendicular directions, and the mean value was calculated. Hyphal morphology was examined using a coverslip culture method. Oval conidial suspensions were prepared for each strain. One milliliter of conidial suspension was mixed with 25 mL of molten PDA and poured into Petri dishes. After solidification, sterile coverslips were inserted into the medium and incubated at 28°C. Samples were collected at 3, 5, and 7 days post-inoculation (dpi), and hyphal morphology was observed under a microscope.

2.5 Calcofluor white (CFW) staining

CFW staining was performed as described previously (Gao et al., 2023). Briefly, mycelial plugs of each strain were cultured on a slide at 28°C for 3 days. Hyphae were then stained with CFW solution prepared by mixing 1 g/L CFW stock and 1 mol/L NaOH at a 1:1 (v/v) ratio. After staining for 5 min in the dark, samples were examined under a fluorescence microscope to observe hyphal cell walls and septum distribution.

2.6 Conidial production, germination, and appressorium formation

For oval conidial production, five mycelial plugs (5 mm in diameter) were excised from colony margins and inoculated into PDB. Cultures were shaken at 28°C, and samples were collected after 3, 5, and 7 days of incubation. Following filtration to remove mycelia, conidia were harvested and quantified using a hemocytometer. For falcate conidial production, a single mycelial plug was placed at the center of an OMA plate and incubated at 28°C for 14 days. Conidia were harvested by washing the culture surface with sterile water, followed by filtration and hemocytometer counting. The morphology of both conidial types was observed under a microscope.

For oval conidial germination assays, conidial suspensions were adjusted to 1×10^6 conidia/mL, and 20 µL aliquots were placed on clean glass slides. After incubation at 28°C under high-humidity conditions for 6 h, germination was assessed, and the germination rate was calculated. For falcate conidia, which were harvested from 14-day-old OMA cultures and adjusted to 5×10^5 conidia/mL, 20 µL aliquots were deposited onto the surface of healthy maize leaves. Following incubation at 28°C with high humidity for 12 h, conidial germination and appressorium formation were examined.

2.7 Pathogenicity assays

Maize leaves were inoculated with either mycelial plugs or falcate conidial suspensions under both wounded and intact conditions. For wounded inoculation, leaves were first punctured with a sterile

needle before applying the inoculum; for intact inoculation, the inoculum was placed directly onto the leaf surface without any physical damage. For mycelial plug inoculation, fresh 5-mm mycelial plugs were placed with the mycelial side in contact with the leaf surface, with sterile PDA plugs serving as controls. For conidial inoculation, suspensions were adjusted to 5×10^5 conidia/mL, and 20 μL aliquots were applied to the leaf surface, with sterile water as the control. After inoculation, leaves were incubated at 28°C under high-humidity conditions for 3 days, after which lesion development was observed and measured.

2.8 RNA sequencing

To investigate the global transcriptional response to *Cgrubr1* deletion, RNA-Seq was performed on CgrWT and Δ*Cgrubr1* strains. Each strain was cultivated on PDA at 28°C for 3 days, followed by mycelial collection for total RNA isolation. Three independent biological replicates were prepared per strain. Paired-end RNA sequencing and library construction were carried out by Tsingke Biotechnology Co., Ltd. (Beijing, China). High-quality reads were subsequently aligned to the *C. graminicola* M1.001 reference genome (GenBank accession: GCF_000149035.1) for sequence alignment and downstream analysis. Data were processed and analyzed according to a previously described method (Li et al., 2017). Differentially expressed genes (DEGs) were subsequently subjected to Gene Ontology (GO) enrichment analysis and Kyoto Encyclopedia of Genes and Genomes (KEGG) pathway enrichment analysis to identify significantly altered biological processes and pathways.

2.9 Statistical analysis

All experiments were independently repeated at least three times, and data are presented as mean ± standard deviation (SD). Statistical significance was determined by one-way analysis of variance (ANOVA) using IBM SPSS Statistics 23, with significance levels set at $P < 0.05$ and $P < 0.01$. Graphs were generated using GraphPad Prism 8.0.

3 Results

3.1 Protein domain and phylogenetic analyses of CgrUbr1

The *Cgrubr1* gene contains a 6,417-bp open reading frame (ORF) encoding a 2,138-amino-acid protein (GenBank: XP_008093299.1). SMART domain analysis revealed that CgrUbr1 harbors zf-UBR and ClpS domains at the N-terminus and a RING domain at the C-terminus, consistent with the canonical architecture of UBR-family RING-type E3 ubiquitin ligases (Fig. 1A). Phylogenetic analysis using the neighbor-joining method showed that CgrUbr1 clustered with Ubr1 homologs from other *Colletotrichum* species, forming a sister clade most closely related to *Colletotrichum higginsianum* Ubr1. Ubr1 homologs from *Colletotrichum fructicola* and *Colletotrichum siamense* constituted an adjacent clade. In contrast, homologs from *Beauveria bassiana*, *Fusarium verticillioides*, *Fusarium graminearum*, *Neurospora crassa*, *Pyricularia oryzae*, and *Aspergillus nidulans* formed distinct branches, while *Saccharomyces cerevisiae* Ubr1 occupied a more divergent position (Fig. 1B).

3.2 Gene deletion and complementation of *Cgrubr1*

To investigate the biological function of CgrUbr1, we generated *Cgrubr1* deletion mutants via homologous recombination (Supplementary Fig. S1A). PCR analysis confirmed the absence of the wild-type allele, as no target fragment was amplified with the internal primer pair *Cgrubr1*F/*Cgrubr1*R, whereas specific products were obtained with the flanking primer pairs *Cgrubr1*UU/PI and *Cgrubr1*DD/PI1. Three independent mutants were isolated and designated Δ*Cgrubr1*-8, Δ*Cgrubr1*-10, and Δ*Cgrubr1*-11 (Supplementary Fig. S1B). For complementation, a DNA fragment encompassing the native promoter and the full-length genomic sequence of *Cgrubr1* was introduced into a Δ*Cgrubr1* mutant. PCR verification confirmed successful integration, yielding the complemented strain Δ*Cgrubr1*-C (Supplementary Fig. S1B).

3.3 CgrUbr1 regulates vegetative growth and hyphal morphology

To examine the effect of CgrUbr1 on vegetative growth, CgrWT, Δ*Cgrubr1* mutants, and the complemented strain Δ*Cgrubr1*-C were inoculated onto PDA, CZ, CM, MM, and OMA media and cultured at 28°C for 5 days. Compared with CgrWT, all three Δ*Cgrubr1* mutants exhibited significantly reduced colony diameters on every medium tested, with the most severe growth inhibition observed on CZ and MM media. On these two media, colony diameters of the mutants were only approximately 13–15% of those of CgrWT. In contrast, the complemented strain Δ*Cgrubr1*-C displayed restored colony morphology and diameters comparable to CgrWT (Fig. 2A and B).

Hyphal morphology was examined using the coverslip culture method at 3, 5, and 7 dpi, and further characterized by CFW staining to visualize cell wall architecture and septum distribution. The hyphae of CgrWT and the complemented strain Δ*Cgrubr1*-C were slender and relatively uniform in width, with regularly spaced septa (Fig. 3A and B). In contrast, Δ*Cgrubr1* mutants developed thickened hyphae with localized swelling as early as 3 dpi; this segmental swelling became more pronounced over time, progressing to distinct bead-like structures by 5 and 7 dpi (Fig. 3A). CFW staining revealed that distinct fluorescent transverse septa were clearly visible between adjacent swollen regions, with septa in the mutants being more densely distributed than in CgrWT, resulting in an overall bead-like arrangement (Fig. 3B). These results indicate that CgrUbr1 deletion not only significantly inhibits vegetative growth, but also causes severe abnormalities in hyphal morphogenesis and disrupts normal septal patterning.

3.4 CgrUbr1 regulates conidial production and morphology

C. graminicola produces two distinct types of asexual conidia, oval and falcate conidia. To assess the role of CgrUbr1 in conidiation, conidial yields of both types were quantified for each strain. Following culture in PDB for 3, 5, and 7 d, oval conidial yields of the Δ*Cgrubr1* mutants were significantly lower than those of CgrWT at all time points (Fig. 4A). After 14 d of culture on OMA, CgrWT produced 2.48×10^8 falcate conidia per plate, whereas the Δ*Cgrubr1* mutants yielded an average of only 3.48×10^6 conidia

per plate, approximately 1.40% of the wild-type yield (Fig. 4B). The morphology of both conidial types was further examined. Oval conidia of CgrWT were predominantly regular oval to short rod–shaped and relatively uniform in size, whereas conidia of the Δ*Cgrubr1* mutants were markedly swollen, nearly spherical, and variable in size. The falcate conidia of CgrWT were distinctly curved and relatively stout, while those of the Δ*Cgrubr1* mutants were more slender and less curved (Fig. 4C). These results indicate that *Cgrubr1* deletion not only impairs conidial production but also causes pronounced alterations in conidial morphology.

3.5 CgrUbr1 regulates conidial germination and appressorium formation

To examine the effect of CgrUbr1 on conidial germination, oval conidial suspensions of each strain were placed as droplets on clean glass slides and incubated at 28°C under humid conditions for 6 h, after which germination rates were determined. The germination rates of CgrWT and Δ*Cgrubr1*-C were 87.53% and 81.58%, respectively, and germ tubes were readily observed. In contrast, the germination rates of all three Δ*Cgrubr1* mutants were below 1%, and most mutant conidia failed to form germ tubes (Fig. 5A and B). Germination and appressorium formation of falcate conidia were further examined. Falcate conidial suspensions from each strain were inoculated onto maize leaf surfaces and incubated for 12 h. CgrWT and Δ*Cgrubr1*-C formed appressoria normally, whereas typical appressoria were not observed in any of the Δ*Cgrubr1* mutants (Fig. 5A and C). These results demonstrate that *Cgrubr1* deletion impairs germination of both conidial types and completely abolishes normal appressorium formation by falcate conidia.

3.6 CgrUbr1 regulates pathogenicity

To evaluate the role of CgrUbr1 in pathogenicity, maize leaves were inoculated with mycelial plugs or falcate conidial suspensions from each strain under wounded and intact conditions. At 3 dpi, the mycelial plugs from CgrWT and Δ*Cgrubr1*-C produced distinct lesions on both wounded and intact leaves. In contrast, Δ*Cgrubr1* mutants caused only small lesions on wounded leaves, with lesion diameters significantly smaller than those of CgrWT, and produced no visible lesions on intact leaves (Fig. 6A and B). Similar results were obtained with falcate conidial suspensions. CgrWT and Δ*Cgrubr1*-C induced lesions on both leaf conditions, whereas Δ*Cgrubr1* mutants generated only minute lesions on wounded leaves and no detectable lesions on intact leaves (Fig. 6C and D). These findings demonstrate that deletion of *Cgrubr1* severely compromises the pathogenicity of *C. graminicola* on maize, with a near-complete loss of virulence on intact leaves.

3.7 Transcriptome analysis

To further analyze transcriptional changes associated with *Cgrubr1* deletion, RNA-Seq was performed on CgrWT and the Δ*Cgrubr1* mutant. Using CgrWT as the control, a total of 3,136 differentially expressed genes (DEGs) were identified, comprising 1,839 upregulated and 1,297 downregulated genes. GO

enrichment analysis revealed that these DEGs were predominantly associated with functional categories including extracellular region, oxidoreductase activity, fungal-type vacuole, secondary metabolite biosynthetic process, carbohydrate metabolic process, and fatty acid metabolic process (Fig. 7A). KEGG pathway analysis indicated significant enrichment in peroxisome, amino sugar and nucleotide sugar metabolism, fatty acid metabolism, DNA replication, and fatty acid degradation (Fig. 7B).

Further analysis of the major enriched pathways revealed that the DNA replication pathway contained 15 DEGs, of which 14 were downregulated. Notably, DNA replication licensing-related genes, including Mcm2, Mcm4, Mcm5, Mcm6, and Mcm7, were downregulated. In the amino sugar and nucleotide sugar metabolism pathway, multiple genes associated with chitin metabolism were identified, encompassing chitin synthases, chitinases, and chitin deacetylases involved in chitin synthesis, degradation, and deacetylation. Among these, chitin synthesis-related genes were predominantly downregulated, whereas genes implicated in chitin degradation and deacetylation exhibited both up- and down-regulation.

Based on the major phenotypes of the Δ*Cgrubr1* mutant and functional gene annotations, several representative DEGs were further selected for analysis. Additionally, several genes involved in the degradation of plant surface and cell wall components exhibited reduced expression, such as the pectate lyase E-like gene *GLRG_11725*, cutinase gene *GLRG_02128*, GH61/AA9 lytic polysaccharide monooxygenase gene *GLRG_10700*, and GH10 endo-1,4-β-xylanase gene *GLRG_08165* (Table 1).

Table 1
Expression of selected DEGs in Δ*Cgrubr1*

Functional classification	Reference Gene ID	Gene function annotation	Log_2(Δ*Cgrubr1*/ CgrWT)
DNA replication	GLRG_05772	DNA replication licensing factor Mcm6	−1.62
	GLRG_03529	DNA replication licensing factor Mcm2	−1.21
	GLRG_01407	DNA replication licensing factor Mcm4	−1.24
Chitin metabolism	GLRG_05787	Chitin synthase 2-like	−1.46
	GLRG_02726	Class VII chitin synthase	−1.10
	GLRG_02468	Endochitinase A1-like	−1.92
	GLRG_02890	GH18 chitinase-like	+ 4.37
	GLRG_11238	Chitin deacetylase-like	−1.91
	GLRG_11148	Chitin deacetylase / polysaccharide deacetylase-like	+ 5.29
Infection-related processes	GLRG_11725	Pectate lyase E-like	−8.91
	GLRG_02128	Cutinase	−1.33
	GLRG_10700	GH61/AA9 lytic polysaccharide monooxygenase	−3.59
	GLRG_08165	GH10 endo-1,4-β-xylanase	−3.33

4 Discussion

Ubr1 is a key E3 ubiquitin ligase in the N-degron pathway that plays essential roles in fungal growth and development. In this study, we characterized the biological functions of CgrUbr1 in *C. graminicola*. Deletion of *Cgrubr1* inhibited vegetative growth, caused pronounced hyphal swelling and bead-like morphology, and led to severe defects in conidial production, germination, appressorium formation, and pathogenicity. Transcriptome analysis further revealed that *Cgrubr1* deletion was accompanied by altered expression of multiple genes associated with DNA replication, chitin metabolism, and host infection, suggesting that CgrUbr1 orchestrates these processes through the ubiquitin-proteasome system.

Deletion of *Cgrubr1* significantly inhibited vegetative growth in *C. graminicola*. This phenotype is consistent with previous observations that deletion of *Ubl1* (*Ubr1* homolog) in *F. verticillioides* impairs hyphal growth and causes morphological abnormalities, underscoring the conserved role of Ubr1 in

fungal vegetative development (Ridenour et al., 2014). Transcriptome analysis revealed that the DNA replication pathway was strongly affected, with 14 of 15 DEGs being downregulated, including core components of the MCM2–7 complex (*Mcm2*, *Mcm4*, *Mcm5*, *Mcm6*, and *Mcm7*). The MCM2–7 complex forms the core of the eukaryotic replicative helicase, which is essential for DNA replication initiation and replication-fork progression (Bochman & Schwacha, 2009). In *Saccharomyces cerevisiae*, disruption of key functional domains in *Mcm2* or *Mcm6* compromises DNA replication initiation and cell growth (Fang et al., 2016), and aberrant SUMOylation of the MCM complex suppresses replication initiation and causes a slow-growth phenotype (Wei & Zhao, 2016). Collectively, these findings suggest that *Cgrubr1* deletion impairs vegetative growth, at least in part, by downregulating MCM complex genes and compromising DNA replication licensing.

In addition to the reduced growth rate, prolonged culture of Δ*Cgrubr1* mutants led to progressive segmental hyphal swelling and a bead-like arrangement, accompanied by denser septal distribution. Chitin biosynthesis is closely linked to normal hyphal growth and maintenance of hyphal morphology in filamentous fungi. In *C. graminicola*, mutation of *chsA* causes apical hyphal swelling and weakens cell wall integrity (Amnuaykanjanasin & Epstein, 2003). Deletion of *CgChsV* severely impairs vegetative growth and produces markedly enlarged, spherical hyphae (Werner et al., 2007). KEGG enrichment analysis revealed significant enrichment of amino sugar and nucleotide sugar metabolism, and multiple genes participating in chitin synthesis, degradation, and deacetylation displayed altered expression. The chitin synthesis genes *GLRG_05787* and *GLRG_02726* were downregulated, while genes implicated in chitin degradation and deacetylation showed mixed up- and down-regulation. Beyond chitin metabolic genes, the *MoMyo2* homolog *GLRG_02452* was also downregulated in the Δ*Cgrubr1* mutant. In *Magnaporthe oryzae*, deletion of *MoMyo2* suppresses hyphal growth and causes aberrant septum formation, and deletion of *FgMyo2* produces similar defects in *Fusarium graminearum* (Guo et al., 2017; Song et al., 2013).

Conidia are essential for asexual reproduction and dissemination in *C. graminicola*. Deletion of *Cgrubr1* markedly reduced the production of both oval and falcate conidia, with a particularly severe reduction in falcate conidiation, and also caused distinct morphological abnormalities in both spore types. Previous studies have shown that Ubr1 homologs are involved in asexual development in several filamentous fungi. In *F. verticillioides*, deletion of *Ubl1* impairs conidial formation, and alters hyphal morphology and pigment deposition (Ridenour et al., 2014). In *B. bassiana*, *ubr1* deletion severely reduces aerial conidiation and blastospore production in liquid culture, accompanied by markedly downregulated expression of the central developmental regulators *brlA*, *abaA*, and *wetA* (Wang et al., 2021). In *Magnaporthe oryzae*, deletion of *Moubr1* reduces conidial yield by approximately 68% and decreases the number of conidia formed on conidiophores (Shi et al., 2016). Collectively, these studies establish that Ubr1 family members play pivotal and evolutionarily conserved roles in governing asexual sporulation in filamentous fungi.

Conidial germination and appressorium formation are critical early steps in the infection-related development of *C. graminicola*. Following *Cgrubr1* deletion, oval conidia rarely germinated on glass

slides, and falcate conidia failed to germinate normally or produce typical appressoria on maize leaves. Transcriptome analysis revealed that the NoxR-like gene *GLRG_00411* was downregulated in the Δ*Cgrubr1* mutant. The NADPH oxidase (Nox) complex is known to regulate infection-structure development in *Colletotrichum*; for instance, deletion of *CgNOXR* in *C. gloeosporioides* impairs appressorium formation and subsequent infectious hyphal growth, while also disrupting ROS distribution and F-actin organization within appressoria (Liu et al., 2022). Beyond ROS regulation, lipid mobilization and peroxisomal metabolism are intimately linked to appressorium development. Deletion of *ClaPEX6* in *Colletotrichum lagenarium* blocks fatty acid utilization and compromises appressorium formation and pathogenicity (Kimura et al., 2001), and in *Magnaporthe oryzae*, peroxisomal fatty acid β-oxidation is essential for appressorium maturation and plant infection (Wang et al., 2007). Consistently, KEGG analysis of our RNA-Seq data showed significant enrichment of peroxisome, fatty acid degradation, and fatty acid metabolism pathways. Collectively, these results indicate that *Cgrubr1* deletion severely disrupts early infection-related morphogenesis and is accompanied by transcriptional remodeling of genes involved in NADPH oxidase activity and lipid catabolism, underscoring the importance of CgrUbr1 in coordinating the cellular reprogramming required for successful host invasion.

Pathogenicity assays demonstrated that Δ*Cgrubr1* mutants essentially failed to produce visible lesions on intact maize leaves and formed significantly smaller lesions than CgrWT even under wounded conditions. Appressoria are critical infection structures in *C. graminicola* that mediate host penetration (Nordzieke et al., 2019). The inability of Δ*Cgrubr1* falcate conidia to germinate normally and form typical appressoria is therefore a major factor contributing to the severe attenuation of pathogenicity. Beyond penetration defects, successful colonization requires the coordinated expression of enzymes that degrade host surface and cell wall components. During *Colletotrichum* infection, genes encoding such enzymes show stage-specific expression and facilitate tissue invasion (O'Connell et al., 2012). In the Δ*Cgrubr1* mutant, several of these genes were downregulated, including the pectate lyase E-like gene *GLRG_11725*, cutinase gene *GLRG_02128*, GH61/AA9 lytic polysaccharide monooxygenase gene *GLRG_10700*, and GH10 endo-1,4-β-xylanase gene *GLRG_08165*. Similarly, in *C. graminicola*, deletion of *Cgrcon7* is accompanied by reduced expression of multiple plant cell wall–degrading enzyme genes and attenuated virulence (Zhou et al., 2024). In *Colletotrichum coccodes*, deletion of *CcpelA* reduces pectate lyase secretion and extracellular activity, weakening tomato fruit infection (Ben-Daniel et al., 2012). Thus, the downregulation of these host-barrier-degrading enzymes likely further compromises the mutant's ability to invade and colonize plant tissues. Collectively, these findings indicate that CgrUbr1 governs multiple stages of the infection cycle, from appressorium-mediated penetration to plant cell wall degradation, and is therefore indispensable for the full pathogenicity of *C. graminicola*.

In summary, this study systematically analyzed the biological function of the RING-type E3 ubiquitin ligase CgrUbr1 in *C. graminicola*. Phenotypic analyses showed that CgrUbr1 plays important roles in vegetative growth, asexual development, and virulence in *C. graminicola*. In particular, deletion of *Cgrubr1* markedly affected the morphogenesis of hyphae and both conidial types. Transcriptome analysis showed marked changes in the expression of genes associated with DNA replication, chitin metabolism, and host infection, providing transcriptional clues for the related phenotypes. These findings advance

our understanding of Ubr1 function in filamentous phytopathogens, delineate the roles of CgrUbr1 in morphogenesis and pathogenicity, and lay the groundwork for dissecting its underlying molecular mechanisms.

Declarations

Declaration of competing interest

The authors declare that they have no known competing financial interests or personal relationships that could have appeared to influence the work reported in this paper.

Funding

This work was financially supported by the National Natural Science Foundation of China (32560351 and 32660053), and the Natural Science Foundation of Hainan Province (325RC641).

Data availability

Data will be made available on request.

Author statement

Sheng Li: Data curation, Formal analysis, Investigation, Writing - Original Draft. **Min Li**: Formal analysis, Validation. **Zhihui He**: Formal analysis, Investigation. **Qin Lei**: Investigation, Validation. **Zhiqiang Liu**: Conceptualization, Funding acquisition, Supervision, Writing - review & editing. **Xiaoyu Li**: Conceptualization, Funding acquisition, Methodology, Supervision.

References

1. Amnuaykanjanasin, A., & Epstein, L. (2003). A class V chitin synthase gene, *chsA* is essential for conidial and hyphal wall strength in the fungus *Colletotrichum graminicola* (*Glomerella graminicola*). *Fungal Genetics and Biology*, *38*(3), 272–285. https://doi.org/10.1016/S1087-1845(02)00563-7
2. Ben-Daniel, B. H., Bar-Zvi, D., & Tsror, L. (2012). Pectate lyase affects pathogenicity in natural isolates of *Colletotrichum coccodes* and in *pelA* gene-disrupted and gene-overexpressing mutant lines. *Molecular Plant Pathology*, *13*(2), 187–197. https://doi.org/10.1111/j.1364-3703.2011.00740.x
3. Bergstrom, G. C., & Nicholson, R. L. (1999). The biology of corn anthracnose: Knowledge to exploit for improved management. *Plant Disease*, *83*(7), 596–608. https://doi.org/10.1094/PDIS.1999.83.7.596

4. Bochman, M. L., & Schwacha, A. (2009). The Mcm complex: Unwinding the mechanism of a replicative helicase. *Microbiology and Molecular Biology Reviews*, *73*(4), 652–683. https://doi.org/10.1128/MMBR.00019-09
5. Cao, C., & Xue, C. (2021). More than just cleaning: Ubiquitin-mediated proteolysis in fungal pathogenesis. *Frontiers in Cellular and Infection Microbiology*, *11*, 774613. https://doi.org/10.3389/fcimb.2021.774613
6. Dean, R., Van Kan, J. A. L., Pretorius, Z. A., Hammond-Kosack, K. E., Di Pietro, A., Spanu, P. D., Rudd, J. J., Dickman, M., Kahmann, R., Ellis, J., & Foster, G. D. (2012). The Top 10 fungal pathogens in molecular plant pathology. *Molecular Plant Pathology*, *13*(4), 414–430. https://doi.org/10.1111/j.1364-3703.2011.00783.x
7. Du, F., Navarro-Garcia, F., Xia, Z., Tasaki, T., & Varshavsky, A. (2002). Pairs of dipeptides synergistically activate the binding of substrate by ubiquitin ligase through dissociation of its autoinhibitory domain. *Proceedings of the National Academy of Sciences of the United States of America*, *99*(22), 14110–14115. https://doi.org/10.1073/pnas.172527399
8. Fang, D., Cao, Q., & Lou, H. (2016). Sld3-MCM interaction facilitated by Dbf4-dependent kinase defines an essential step in eukaryotic DNA replication initiation. *Frontiers in Microbiology*, *7*, 885. https://doi.org/10.3389/fmicb.2016.00885
9. Finley, D., Ulrich, H. D., Sommer, T., & Kaiser, P. (2012). The ubiquitin-proteasome system of *Saccharomyces cerevisiae*. *Genetics*, *192*(2), 319–360. https://doi.org/10.1534/genetics.112.140467
10. Gao, J., Zhou, S., Tang, W., Wang, J., Liu, H., Zhang, Y., Wang, L., Li, X., & Liu, Z. (2023). The velvet proteins CsVosA and CsVelB coordinate growth, cell wall integrity, sporulation, conidial viability and pathogenicity in the rubber anthracnose fungus *Colletotrichum siamense*. *Microbiological Research*, *268*, 127290. https://doi.org/10.1016/j.micres.2022.127290
11. Guo, M., Tan, L., Nie, X., & Zhang, Z. (2017). A class-II myosin is required for growth, conidiation, cell wall integrity and pathogenicity of *Magnaporthe oryzae*. *Virulence*, *8*(7), 1335–1354. https://doi.org/10.1080/21505594.2017.1323156
12. Hwang, C. S., Shemorry, A., Auerbach, D., & Varshavsky, A. (2010). The N-end rule pathway is mediated by a complex of the RING-type Ubr1 and HECT-type Ufd4 ubiquitin ligases. *Nature Cell Biology*, *12*(12), 1177–1185. https://doi.org/10.1038/ncb2121
13. Kimura, A., Takano, Y., Furusawa, I., & Okuno, T. (2001). Peroxisomal metabolic function is required for appressorium-mediated plant infection by *Colletotrichum lagenarium*. *The Plant Cell*, *13*(8), 1945–1957. https://doi.org/10.1105/TPC.010084
14. Li, G., Qi, X., Sun, G., Rocha, R. O., Segal, L. M., Downey, K. S., Wright, J. D., & Wilson, R. A. (2020). Terminating rice innate immunity induction requires a network of antagonistic and redox-responsive E3 ubiquitin ligases targeting a fungal sirtuin. *New Phytologist*, *226*(2), 523–540. https://doi.org/10.1111/nph.16365
15. Li, X., Wu, Y., Liu, Z., & Zhang, C. (2017). The function and transcriptome analysis of a bZIP transcription factor CgAP1 in *Colletotrichum gloeosporioides*. *Microbiological Research*, *197*, 39–48.

https://doi.org/10.1016/j.micres.2017.01.006

16. Lin, S., Wei, H., Guo, C., Tang, W., Liu, Z., & Li, X. (2025). Biological functions of a C2H2-type transcription factor CgrFlbC in *Colletotrichum graminicola*. *Microbiology China*, *52*(4), 1507–1519. https://doi.org/10.13344/j.microbiol.china.240636. (in Chinese).
17. Liu, N., Wang, W., He, C., Luo, H., An, B., & Wang, Q. (2022). NADPH oxidases play a role in pathogenicity via the regulation of F-actin organization in *Colletotrichum gloeosporioides*. *Frontiers in Cellular and Infection Microbiology*, *12*, 845133. https://doi.org/10.3389/fcimb.2022.845133
18. Mims, C. W., & Vaillancourt, L. J. (2002). Ultrastructural characterization of infection and colonization of maize leaves by *Colletotrichum graminicola*, and by a *C. graminicola* pathogenicity mutant. *Phytopathology*, *92*(7), 803–812. https://doi.org/10.1094/PHYTO.2002.92.7.803
19. Nordzieke, D. E., Sanken, A., Antelo, L., Raschke, A., Deising, H. B., & Pöggeler, S. (2019). Specialized infection strategies of falcate and oval conidia of *Colletotrichum graminicola*. *Fungal Genetics and Biology*, *133*, 103276. https://doi.org/10.1016/j.fgb.2019.103276
20. O'Connell, R. J., Thon, M. R., Hacquard, S., Amyotte, S. G., Kleemann, J., Torres, M. F., Damm, U., Buiate, E. A., Epstein, L., Alkan, N., Altmüller, J., Alvarado-Balderrama, L., Bauser, C. A., Becker, C., Birren, B. W., Chen, Z., Choi, J., Crouch, J. A., Duvick, J. P., & Vaillancourt, L. J. (2012). Lifestyle transitions in plant pathogenic *Colletotrichum* fungi deciphered by genome and transcriptome analyses. *Nature Genetics*, *44*(9), 1060–1065. https://doi.org/10.1038/ng.2372
21. Panaccione, D. G., Vaillancourt, L. J., & Hanau, R. M. (1989). Conidial dimorphism in *Colletotrichum graminicola*. *Mycologia*, *81*(6), 876–883. https://doi.org/10.1080/00275514.1989.12025677
22. Ranum, P., Peña-Rosas, J. P., & Garcia-Casal, M. N. (2014). Global maize production, utilization, and consumption. *Annals of the New York Academy of Sciences*, *1312*(1), 105–112. https://doi.org/10.1111/nyas.12396
23. Ridenour, J. B., Smith, J. E., Hirsch, R. L., Horevaj, P., Kim, H., Sharma, S., & Bluhm, B. H. (2014). UBL1 of *Fusarium verticillioides* links the N-end rule pathway to extracellular sensing and plant pathogenesis. *Environmental Microbiology*, *16*(7), 2004–2022. https://doi.org/10.1111/1462-2920.12333
24. Rudolph, A. Y., Schunke, C., Sasse, C., Antelo, L., Gerke, J., Braus, G. H., Pöggeler, S., & Nordzieke, D. E. (2025). Maize diterpenoid sensing via the Ste3 A-pheromone receptor guide oval conidia of *Colletotrichum graminicola* to host roots. *Molecular Plant Pathology*, *26*(9), e70155. https://doi.org/10.1111/mpp.70155
25. Shi, H. B., Chen, G. Q., Chen, Y. P., Dong, B., Lu, J. P., Liu, X. H., & Lin, F. C. (2016). MoRad6-mediated ubiquitination pathways are essential for development and pathogenicity in *Magnaporthe oryzae*. *Environmental Microbiology*, *18*(11), 4170–4187. https://doi.org/10.1111/1462-2920.13515
26. Shi, H. B., Chen, N., Zhu, X. M., Liang, S., Li, L., Wang, J. Y., Lu, J. P., Lin, F. C., & Liu, X. H. (2019). F-box proteins MoFwd1, MoCdc4 and MoFbx15 regulate development and pathogenicity in the rice blast fungus *Magnaporthe oryzae*. *Environmental Microbiology*, *21*(8), 3027–3045. https://doi.org/10.1111/1462-2920.14699

27. Song, B., Li, H. P., Zhang, J. B., Wang, J. H., Gong, A. D., Song, X. S., Chen, T., & Liao, Y. C. (2013). Type II myosin gene in *Fusarium graminearum* is required for septation, development, mycotoxin biosynthesis and pathogenicity. *Fungal Genetics and Biology*, *54*, 60–70. https://doi.org/10.1016/j.fgb.2013.02.010
28. Sukno, S. A., García, V. M., Shaw, B. D., & Thon, M. R. (2008). Root infection and systemic colonization of maize by *Colletotrichum graminicola*. *Applied and Environmental Microbiology*, *74*(3), 823–832. https://doi.org/10.1128/AEM.01165-07
29. Tasaki, T., Sriram, S. M., Park, K. S., & Kwon, Y. T. (2012). The N-end rule pathway. *Annual Review of Biochemistry*, *81*, 261–289. https://doi.org/10.1146/annurev-biochem-051710-093308
30. Turner, G. C., Du, F., & Varshavsky, A. (2000). Peptides accelerate their uptake by activating a ubiquitin-dependent proteolytic pathway. *Nature*, *405*(6786), 579–583. https://doi.org/10.1038/35014629
31. Wang, D. Y., Mou, Y. N., Du, X., Guan, Y., & Feng, M. G. (2021). Ubr1-mediated ubiquitylation orchestrates asexual development, polar growth, and virulence-related cellular events in *Beauveria bassiana*. *Applied Microbiology and Biotechnology*, *105*(7), 2747–2758. https://doi.org/10.1007/s00253-021-11222-0
32. Wang, J., Zhou, S., Zhang, Y., Lin, S., Yu, J. H., Liu, Z., & Li, X. (2025). The GATA transcription factor NsdD regulates vegetative growth, asexual sporulation, and melanin biosynthesis in *Colletotrichum siamense* and *C. graminicola*. *Phytopathology*, *115*(12), 1681–1694. https://doi.org/10.1094/PHYTO-07-25-0238-R
33. Wang, Z. Y., Soanes, D. M., Kershaw, M. J., & Talbot, N. J. (2007). Functional analysis of lipid metabolism in *Magnaporthe grisea* reveals a requirement for peroxisomal fatty acid β-oxidation during appressorium-mediated plant infection. *Molecular Plant-Microbe Interactions*, *20*(5), 475–491. https://doi.org/10.1094/MPMI-20-5-0475
34. Wei, L., & Zhao, X. (2016). A new MCM modification cycle regulates DNA replication initiation. *Nature Structural & Molecular Biology*, *23*(3), 209–216. https://doi.org/10.1038/nsmb.3173
35. Werner, S., Sugui, J. A., Steinberg, G., & Deising, H. B. (2007). A chitin synthase with a myosin-like motor domain is essential for hyphal growth, appressorium differentiation, and pathogenicity of the maize anthracnose fungus *Colletotrichum graminicola*. *Molecular Plant-Microbe Interactions*, *20*(12), 1555–1567. https://doi.org/10.1094/MPMI-20-12-1555
36. Xia, Z., Webster, A., Du, F., Piatkov, K., Ghislain, M., & Varshavsky, A. (2008). Substrate-binding sites of UBR1, the ubiquitin ligase of the N-end rule pathway. *Journal of Biological Chemistry*, *283*(35), 24011–24028. https://doi.org/10.1074/jbc.M802583200
37. Yang, X., Hu, Z., Yuan, J., Zou, R., Wang, Y., Peng, X., Xu, S., & Xie, C. (2023). Functional role of RING ubiquitin E3 ligase VdBre1 and VdHrd1 in the pathogenicity and penetration structure formation of *Verticillium dahliae*. *Journal of Fungi*, *9*(10), 1037. https://doi.org/10.3390/jof9101037
38. Zhang, Y., Zhou, S., Wang, L., Wei, H., Xie, J., Liu, Z., & Li, X. (2024). A transcription factor CgrStuA regulates vegetative growth, conidial production, germination, and hyphopodium formation of

Colletotrichum graminicola. *Microbiology China*, *51*(8), 3020–3031. https://doi.org/10.13344/j.microbiol.china.230863. (in Chinese).

39. Zheng, N., & Shabek, N. (2017). Ubiquitin ligases: Structure, function, and regulation. *Annual Review of Biochemistry*, *86*, 129–157. https://doi.org/10.1146/annurev-biochem-060815-014922
40. Zhou, S., Liu, S., Guo, C., Wei, H., He, Z., Liu, Z., & Li, X. (2024). The C2H2 transcription factor Con7 regulates vegetative growth, cell wall integrity, oxidative stress, asexual sporulation, appressorium and hyphopodium formation, and pathogenicity in *Colletotrichum graminicola* and *Colletotrichum siamense*. *Journal of Fungi*, *10*(7), 495. https://doi.org/10.3390/jof10070495

Figures

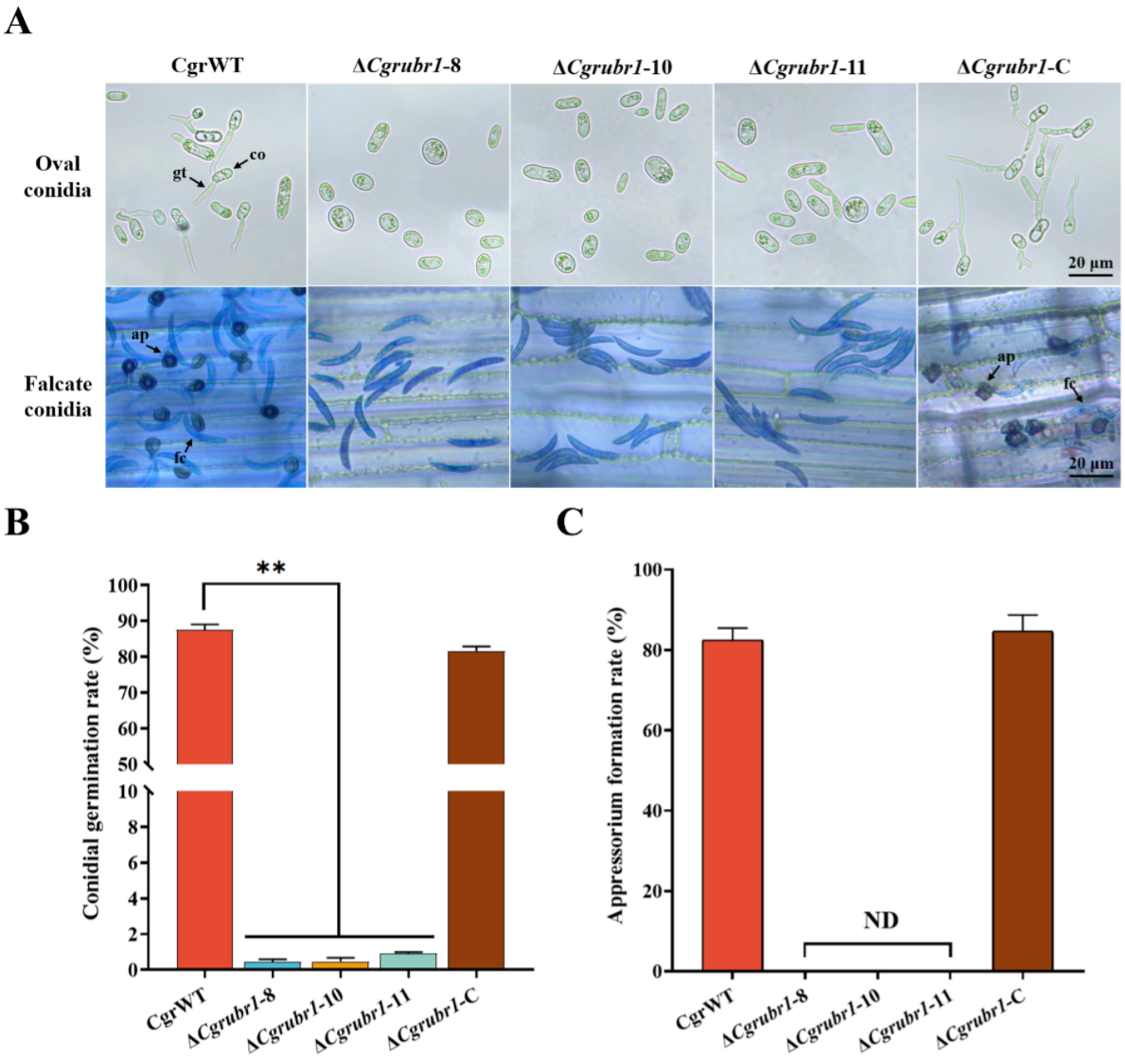


Figure 5

Effects of CgrUbr1 on conidial germination and appressorium formation in *C. graminicola*. (A) Germination of oval conidia and appressorium formation of falcate conidia in the indicated strains. co: oval conidium; gt: germ tube; fc: falcate conidium; ap: appressorium. (B) Statistical analysis of oval conidial germination rates after 6 h of incubation on glass slides. (C) Statistical analysis of appressorium formation rates of falcate conidia after 12 h of incubation on maize leaf surfaces. ND: not detected; **: significance level, $P < 0.01$

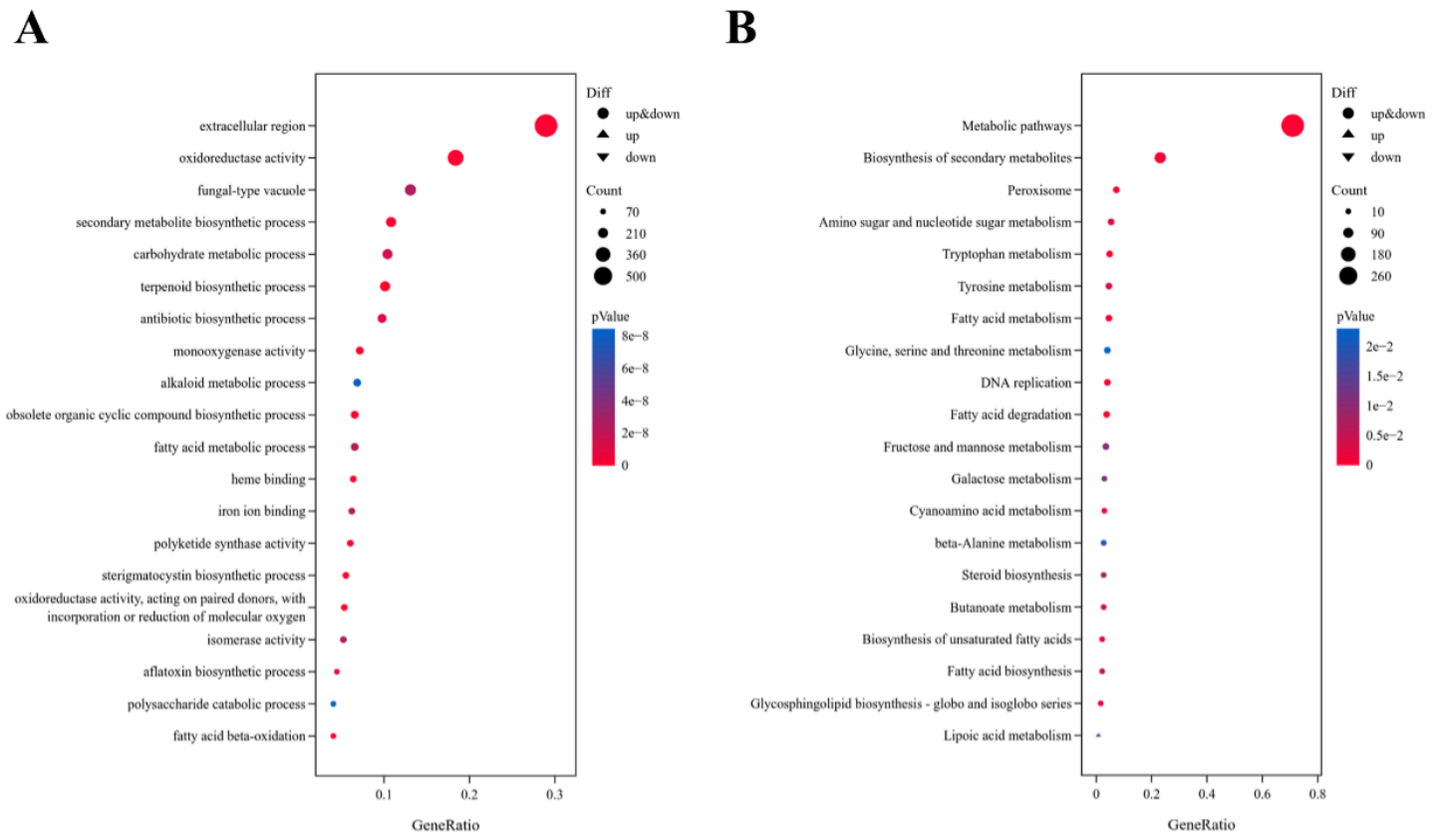


Figure 7

Functional enrichment analysis of differentially expressed genes (DEGs) in the Δ*Cgrubr1* mutant. (A) GO enrichment analysis of DEGs in the Δ*Cgrubr1*mutant. (B) KEGG pathway enrichment analysis of DEGs in the Δ*Cgrubr1* mutant

Supplementary Files

This is a list of supplementary files associated with this preprint. Click to download.

- ESM1.docx